Available online at website: https://journal.bcrec.id/index.php/bcrec

Bulletin of Chemical Reaction Engineering & Catalysis, 19 (1) 2024, 134-140

Research Article

Complex Concentrated Alloy Catalyst of AlCrFeCoNi for Heterogeneous Degradation of Rhodamine B

Kiky Corneliasari Sembiring[1,*], Irgi Ahmad Fahrezi[2], M. Muhdarina[2], Ahmad Afandi[3]

[1]Research Center for Chemistry - BRIN, Building 452 KST BJ Habibie, Serpong, Tangerang Selatan 15314, Indonesia.
[2]Department of Chemistry, Faculty of Mathematics and Natural Sciences, Universitas Riau, Kampus Bina Widya, Km 12.5, Pekanbaru, Riau, Indonesia.
[3]Research Center for Advanced Materials - BRIN, Building 442 KST BJ Habibie, Serpong, Tangerang Selatan 15314, Indonesia.

Received: 2nd January 2024; Revised: 13th February 2024; Accepted: 14th February 2024
Available online: 16th February 2024; Published regularly: April 2024

Abstract

The Fe-based catalysts have attracted good attention due to their earth abundance and low toxicity with good Fenton-like performance. However, the narrow pH working range and iron-containing sludge produced during the reaction drove the necessary of developing a potential catalyst in the corresponding application. High entropy alloy that now expands to complex concentrated alloy (CCA) represents a new class of material owing to a broader range of functional and structural properties. A new application of CCA as a catalyst for catalytic degradation of azo dyes has already been a scientific research hotspot. AlCrFeCoNi CCA powder has been successfully synthesized by mechanical alloying (MA) method using a vertical planetary ball mill. Based on the characterization, the catalyst possessed a spherical morphology with a particle size range of 3.5-12.6 μm. The catalyst exhibited photo-Fenton performance up to 85.3% which would be a promising Fenton-like catalyst for wastewater treatment.

Keywords: complex concentrated alloy (CCA); azo dyes; AlCrFeCoNi; mechanical alloying; ball mill

How to Cite: K.C. Sembiring, I.A. Fahrezi, M. Muhdarina, A. Afandi (2024). Complex Concentrated Alloy Catalyst of AlCrFeCoNi for Heterogeneous Degradation of Rhodamine B. *Bulletin of Chemical Reaction Engineering & Catalysis*, 19 (1), 134-140 (doi: 10.9767/bcrec.20110)

Permalink/DOI: https://doi.org/10.9767/bcrec.20110

1. Introduction

Indonesia is among the world's largest textile manufacturers in the top ten. Indonesia's textile industry accounted for about 6% growth in the manufacturing sector [1]. In the textile industry, the dyeing and finishing steps generated around 17-20% of total wastewater effluent [2]. It has been reported that more than 300.000 tons of dyes are discharged annually into treatment facilities [3].

One of the most widely used chromophores in dye chemistry is azo dyes, accounting for more than 60% of synthetic dyes in the market [4]. The color of azo dyes is determined by the electron-withdrawing functional groups (chromophores), such as N=N, C=O, −CH=N, NO_2, NO, NOH, C=N, C≡N, C=C, and C≡C; and electron-releasing groups (auxochromes), such as SO_3H, OH, COOH, NH_2, NH_3, $NHCH_3$, and $N(CH_3)_2$ groups. The stable structure of dyes present in wastewater makes their degradation difficult. Therefore, it is essential to understand the practical methods to deal with textile wastewater to save the environment.

Various techniques for azo dye removal in wastewater have beeln attempted, such as physical adsorption, chemical and biological degradation, coagulation, and chemical oxidation by Fenton and hypochlorite methods [5–8]. Among those techniques, Fenton method ($Fe^{2+}/Fe^{3+}+H_2O_2$) has been a more effective approach. Its powerful oxidation capability can quickly degrade organic dyes with different

* Corresponding Author.
Email: kiky001@brin.go.id (K.C. Sembiring)

chemical structures (xanthene, thiazine, triarylmethane, and azo dyes) [9,10], but it demands highly acidic conditions. Thus, developing a new type of heterogeneous catalyst is urgently needed for efficient dye degradation and environmental safety.

Over this last decade, high-entropy alloys (HEAs) have received extensive attention and achieved tremendous evolvements in the materials science community. HEA is defined as the five or more principal elements in an equiatomic ratio (concentration between 5-35%) with no distinction between solute and solvent [11,12]. HEAs have been reported to be promising catalysts because of their highly complex atomic structure, high configurational entropy, and potential energy. A new term for complex concentrated alloys (CCA) is an expansion of HEA, which allows elemental concentration of less than 5% or excess than 35%, including single phase intermetallic alloys with any number of intermetallic phases and solid solution [13]. CCA has been commonly synthesized by wet chemistry method, thermal spraying, and mechanical alloying (MA) [14].

CCA of AlCoCrTiZn and AlCrFeMn have been explored and exhibit prominent efficiency in degrading azo dye Direct Blue 6 (DB6). Both research only explored the zero valence metal (ZVM) reduction method for azo groups degradation, not involving a Fenton-like process, which can work for more complicated structures of dyes. The CCA catalysis degradation has yet to be widely studied and the literary studies are limited.

In this work, AlCrFeCoNi CCA synthesized by MA was conducted to study the behaviour of CCA in Fenton-like activity of dye degradation. The elements of Fe, Co, Ni, Cu and Cu have a direct contribution to possessing Fenton-like activity [15]. In contrast while Al and Cr elements were used to promote the formation of amorphous alloys.

Several researchers focused on Fe-based metallic glass catalyst for azo dyes degradation. Although novel HEA has been developed in recent years, but less works reported about dye degradation behaviour of equiatomic HEA and of course the CCA catalyst. This study aims syntesize AlCrFeCoNi CCA by MA process using planetary ball mill and investigate the performance in Fenton-like process dye degradation of Rhodamine B (RhB). In this work, AlCrFeCoNi CCA were successfully prepared by one-step ball milling method and then used as heterogeneous photo-Fenton catalysts. The catalytic performances were investigated by decomposition of RhB, which usually hard to be decomposed by ZVM reduction method.

2. Materials and Methods

2.1 Materials

The quantitative high purity (>99%) precursor metals of Al, Cr, Fe, Co, Ni powders with 15–53 μm particle sizes were used as raw materials to synthesize equiatomic AlCrFeCoNi materials. Stearic acid for process controlling agent (PCA), hydrogen peroxide (H_2O_2, 35%), H_3PO_4, $Na_2S_2O_3$, and RhB were purchased from Merck and used without further purification.

2.2 Catalyst Synthesis

The alloy catalysts of AlCrFeCoNi were synthesized by ball milling using corresponding pure metal powders as raw materials. The mixed pure powders of Al (5.39 g), Cr (10.39 g), Fe (11.17 g), Co (11.79 g), Ni (11.74 g) and the amount of stearic acid (2 wt%) as control agent were loaded into a 500 mL stainless steel jar together with stainless steel balls which have different diameters (5, 8, 10, and 15 mm), among them, the ratio of ball to powder weight ratio was 10:1. The MA process was carried out in the vertical planetary ball mill (TENCAN, Changsa Tianchuang Powder Technology, China) at 300 rpm rotation speed for 60 h. To avoid the phenomenon of overheating, the rotation direction was changed every hour with a pause of 10 min. The synthesized catalyst was then calcined at 400 °C under argon gas.

2.3 Materials Characterization

The crystal structure of the as-milled AlCrFeCoNi CCA powders was analyzed by X-ray diffraction (XRD, Bruker D8 Advance) using Co source. Thermo gravimetric (TG) analysis / Differential Scanning Calorimeter (DSC) was carried out on 60 h milled AlCrFeCoNi CCA powder in Linseis STA Platinum Series of TG/DSC with a heating rate of 10 °C/min from 30 to 1200 °C. The morphology characteristics the samples were investigated by scanning electron microscopy (SEM, Hitachi High-Tech Co. Ltd, Japan).

2.4 Catalytic activity

The catalytic of the as-prepared AlCrFeCoNi CCA was examined for the degradation of RhB at room temperature and various reaction pH. In a typical experiment, the mixture of 50 mL of RhB solution (10 ppm), 1 wt% catalyst, and 1 v% H_2O_2 was magnetically stirred under a UV lamp (λ = 250-400 nm). Before the degradation, the whole suspension was stirred in the dark for 30 min to ensure the establishment of the adsorption-desorption equilibrium). The extent of photocatalytic degradation was evaluated using a

UV–Vis spectrophotometer (Agilent Technology) by measuring the change in maximum absorbance of 554 nm. The photocatalytic degradation efficiency (%) of AlCrFeCoNi CCA at any time t after visible light irradiation was calculated according to the following equation:

$$PDE\% = \frac{C_0 - C_t}{C_0} \times 100 \quad (1)$$

where, PDE is photodegradation efficiency (%), C_0 (mg.L^{-1}) and C_t (mg.L^{-1}) are the concentration of RhB dye in the test solution at initial and after time, respectively.

3. Results and Discussion

3.1 Characterization of AlCrFeCoNi CCA

The AlCrFeCoNi CCA powder was prepared from room temperature MA of high-purity precursor metals through ball milling process with stearic acid, as PCA as illustrated in Figure 1.

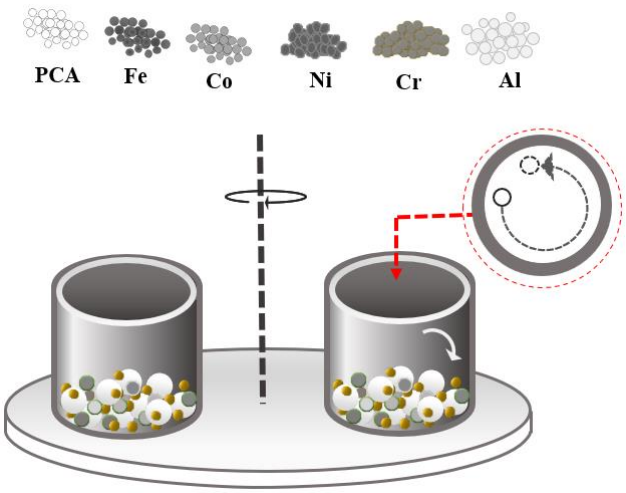

Figure 1. Room temperature ball milling synthesis of CCA AlCrFeCoNi powder.

Differential thermal analysis (DTA) measurements were conducted on 60 h milled AlCrFeCoNi CCA powder samples. Thus, the phase transformation temperatures upon heating can be predicted, especially at the low temperature. Figure 2 shows the DTA and thermographimetric (TG) curves of 60 h mechanically alloyed AlCrFeCoNi CCA powder with a heating rate of 10 °C/min and up to 1200 °C. The slight exothermic curve was observed in a temperature range of about 150 to 300 °C, which may relieve the internal stresses during the high-energy ball milling process. The exothermic peaks above 450 °C, approximately 600 °C, were associated with the energy released during the phase transformation process. Oxidation of metal occurred to form metal oxide which is indicated by the weight gain curve present in TG analysis by heating the sample above 450 °C. To avoid the oxide form of AlCrFeCoNi CCA powder, the calcination process of the catalyst was conducted at 400 °C. In addition, the stearic acid as PCA is decomposed at 361 °C; thus all the PCA can be removed at calcination temperature.

Figure 3 illustrates the SEM morphologies of the AlCrFeCoNi CCA powder and corresponding particle size distribution (Figure 3(a-b)) after treated calcination at 400 °C to remove stearic acid. As revealed in this figure, spherical morphology appeared, and the particle size exhibits a relatively uniform distribution in the range of 3.5-12.6 μm. The catalyst samples with small average particle sizes (less than 20 μm) are caused by the high entropy effects due to the MA process. The milling balls impact the phenomena of dynamic balance between the fracture occurred in individual particles and cold welding among particles. Furthermore, the ductile property Al powders caused the brittle particles occluded and trapped into it. Thus, the particle size cannot reach nano size. These regular patterns suggest

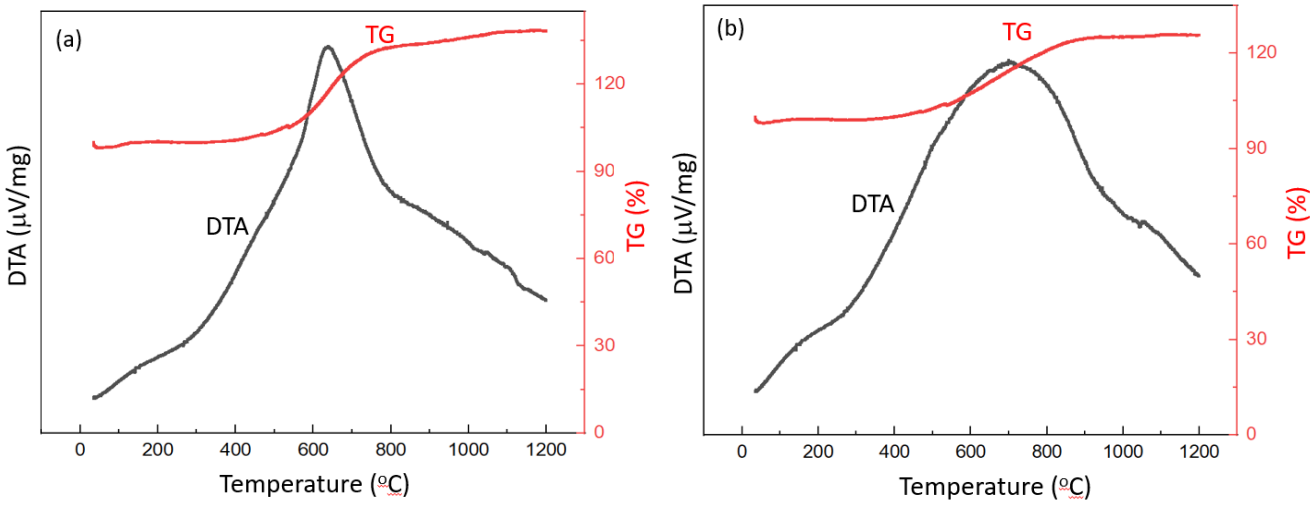

Figure 2. DTA and TG curve of a 60 h milled AlCrFeCoNi CCA powder.

the small particle size and spherical round block morphology are caused by the high entropy effect, thus the catalyst's specific surface area and active sites may expect to significantly increase [16].

The composition of each element in the CCA was quantitatively analyzed by the EDS spectrum of 60 h milled sample (Figure 3(c)). It confirms that the composition is nearly equiatomic. The lower amount of Al element detected through EDS may be caused by its lower atomic mass resulted in less easy to detect. The CCA sample with wide range of atomic numbers, the peak size detectors cannot precisely represent the exact atomic ratio of elements present. However, those EDS results verify that the actual composition of AlCrFeCoNi CCA is close to the nominal equiatomic composition. In Figure 3(d-i) indicates that all five elements (Al, Cr, Fe, Co, Ni) are distributed homogeneously.

The XRD patterns of AlCrFeCoNi CCA are shown in Figure 4, the reduction and broadening of the peaks are attributed to the decrease in crystallite size and diffusion of five elements during milling, leading to the formation of solid solution. The pattern peaks demonstrate simple solid-solution phases (FCC and BCC). The initial five multi phases crystal structure of each element is reduced into two phases after MA process. This phenomenon indicates that the five elements are alloyed during MA process. The lattice parameter of FCC is close to Ni, which may be caused by the Al and Co elements diffusing with Ni to form FCC solid solution. Meanwhile, the lattice parameter of BCC is close to that of Fe and Cr, but the melting point of Cr is higher and is less active in the diffusion. In this case, Cr acts as the solvent in the formation of BCC solid solution [17].

After calcination at 400 °C, the peaks remained similar, except for a small peak (33.5°) that may be the intermetallic of NiAl. The NiAl is generally obtained through liquid-solid-phase transformation via crystal nucleation and subsequent crystal growth [18]. This indicates that solid solution was formed after milling and due to heating treatment under argon at 400 °C, intermetallic of NiAl appeared.

3.2 Degradation of Rhodamine B dye by AlCrFeCoNi CCA

To test the catalyst activity, first, we compare the efficiency of two oxidation processes, Fenton and photo-Fenton. In the Fenton process, a

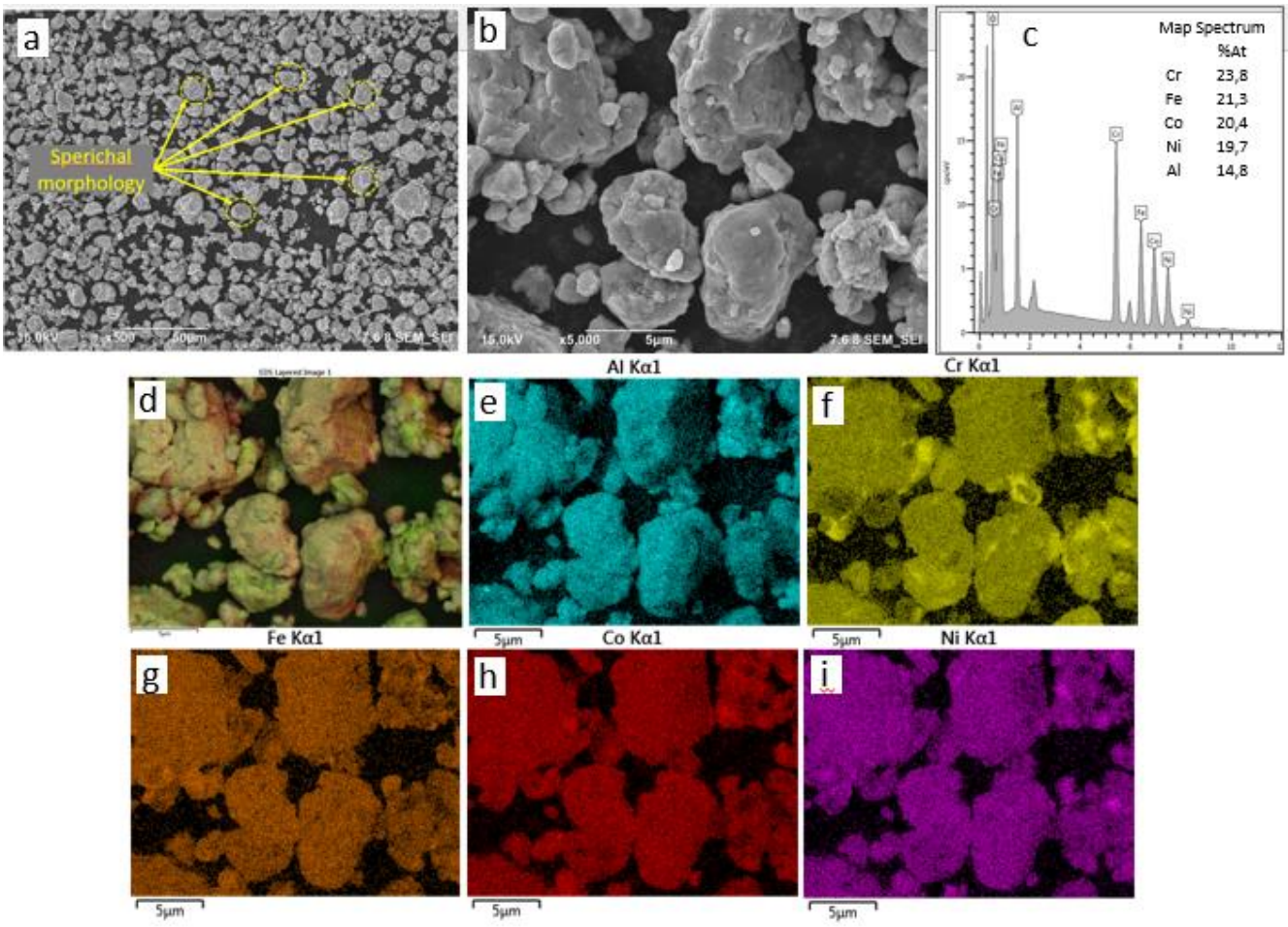

Figure 3. SEM images of AlCrFeCoNi CCA powder: (a, b) under different magnifications; (c) EDS analysis; (d, e, f, g, h, i) elemental distribution mappings of the samples.

mixture of H_2O_2, AlCrFeCoNi CCA, and a model compound of RhB 10 ppm was stirred at room temperature. In the Photo-Fenton process, a similar mixture was stirred at room temperature under *uv* radiation, and the result is found in Figure 5. Photo-Fenton reaction worked more efficiently to degrade RhB with a photodegradation efficiency (PDE) of 85.7%. Under Fenton reaction, the degradation efficiency was about half compared to that of Photo-Fenton. Henceforward, the degradation reaction was conducted in Photo-Fenton reaction.

During the RhB degradation process, a double effect mechanism is occurred on the surface of CCA where the heterogeneous photo-Fenton and semiconductor CCA promote each other. M^{3+} can capture the photo-induced electrons in CCA and it plays role in producing the combination rate of photoelectrons (e^-) and holes (h^+) to increase the photocatalytic activity. This process produces high active ·OH that reveals superior catalytic efficiency and ensures the catalyst's cycle performance. For example, $Fe^{2+}/Co^{2+}/Ni^{2+}$ further reacts with H_2O_2 to generate $Fe^{3+}/Co^{3+}/Ni^{3+}$ utilizing UV light, which can effectively increase the Photo-Fenton. The probable mechanism of the photodegradation of RhB is represented in Figure 6.

The experiment of RhB decomposition carried out catalyzed by AlCrFeCoNi and H_2O_2 as shown in Figure 6. In the decomposition of RhB with only AlCrFeCoNi catalyst (Figure 7(a)) resulted in slight decrease of the intensity peak in absorption spectra. So did the decomposition of RhB catalyzed by H_2O_2 (Figure 7(b)), the intensity peak in the absorption spectra does not decrease a lot. Applying the AlCrFeCoNi catalyst together with H_2O_2 implied that the degradation reaction worked effectively (Figure 7(c)). The photodegradation reaction was also conducted at different pH of 2, 3, and 7 (Figure 7(d)). The Photo-Fenton reaction shows higher activity in an acidic environment to reach up to 97.5% PDE after 60 min reaction time. However, at around neutral conditions, the photodegradation reaction still worked well to give a %PDE of 85.7. Thus, realizing highly efficient degradation of RhB without adjusting reaction conditions at low acidity can avoid secondary pollution to the environment.

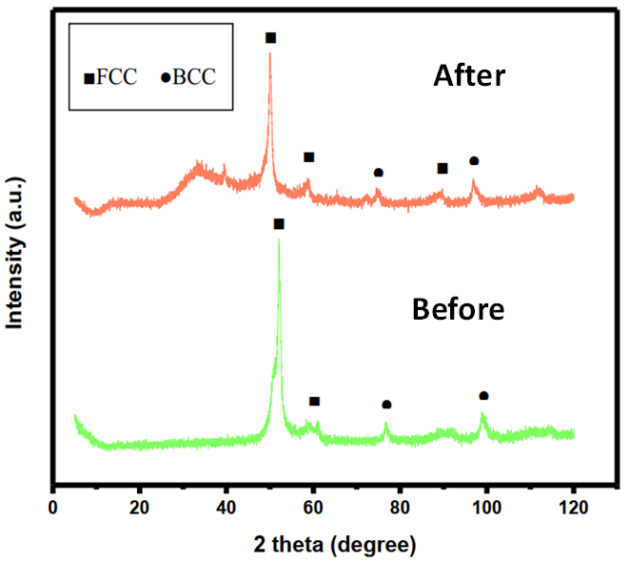

Figure 4. XRD patterns of AlCrFeCoNi CCA powder.

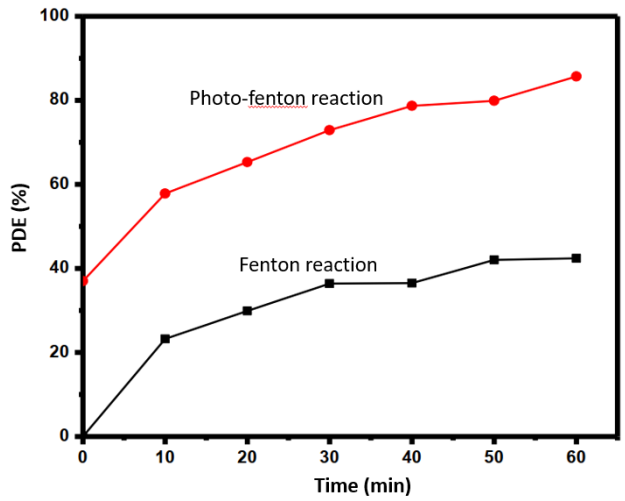

Figure 5. The Fenton and photo-Fenton reaction in degradation RhB.

4. Conclusions

AlCrFeCoNi CCA was successfully synthesized, and the elements alloyed during the MA process as indicated by the formation of simple solid-solution phases (FCC and BCC). This work assessed the capability of AlCrFeCoNi CCA as a catalyst in the degradation of RhB dye in the Photo-Fenton process. The AlCrFeCoNi CCA can

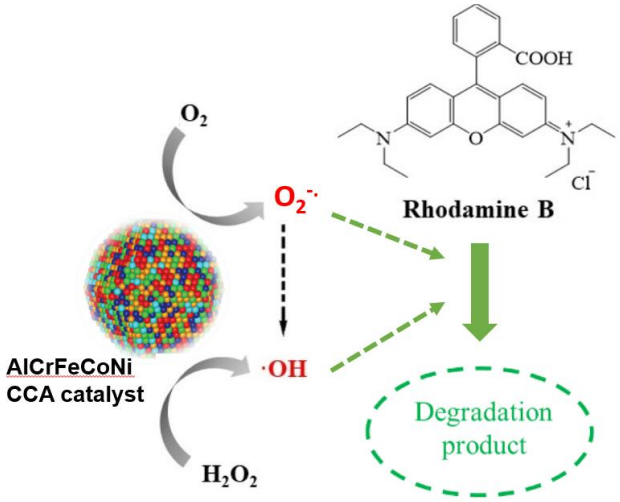

Figure 6. Probable photodegradation mechanism of RhB using AlCrFeCoNi CCA catalyst.

speed up and increase the effectiveness of the process by accelerating the development of hydroxyl radicals. The catalyst exhibited photo-Fenton performance up to 85.3% which would be a promising Fenton-like catalyst for wastewater treatment. The result of this study can be applied in treating RhB dye for wastewater management, especially in the textile industry, to fulfil SDG number 9, clean water and sanitation.

Acknowledgments

The authors acknowledge the Rumah Program The Nanotechnology and Materials Research Organization, Badan Riset dan Inovasi Nasional (ORNM, BRIN) for financial support of this work. We also acknowledge the facilities and technical supports from Advanced Characterisation Laboratories Serpong, National Research and Innovation Agency through E Layanan Sains (ELSA), BRIN.

Credit Author Statement

Author Contribution: *K.C. Sembiring*: conceptualization, methodology, writing – original draft, writing – review & editing, supervision; *I.A. Fahrezi*: formal analysis, investigation; *M. Muhdarina*: supervision, data curation; *A. Afandi*: formal analysis, writing, review and editing. All authors have read and agreed to the published version of the manuscript.

References

[1] Pearl, H. (2022). Indonesia textile industry outlook brightens after COVID blow. Nikkei Asia.

[2] Halepoto, H., Gong, T., Memon, H. (2022). Current status and research trends of textile wastewater treatments—A bibliometric-based study. *Frontiers in Environmental Science*, 10, 1042256. DOI: 10.3389/fenvs.2022.1042256.

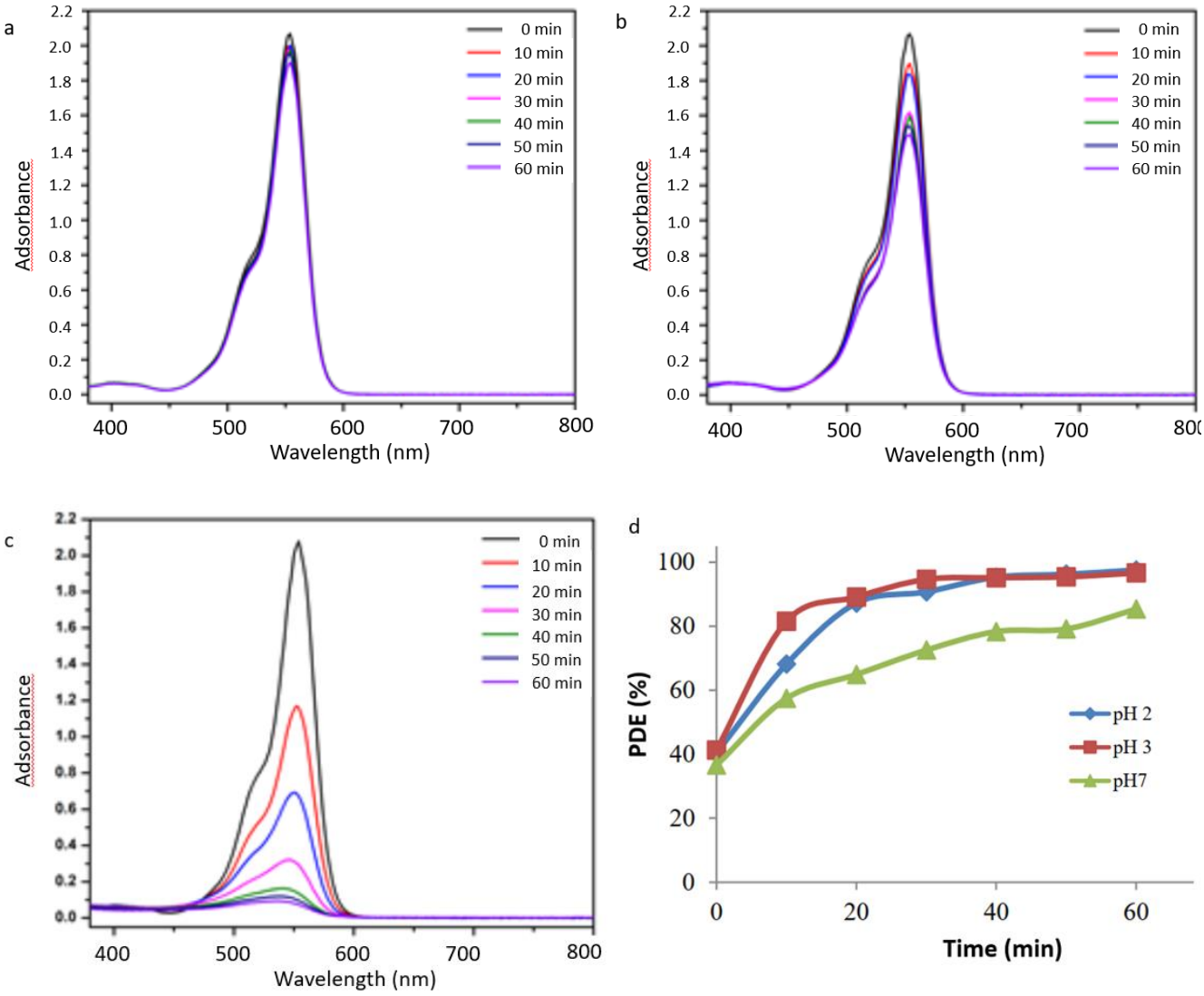

Figure 7. Time dependent UV-vis absorption spectra of RhB solution in the presence of (a) AlCrFeCoNi catalyst and (b) H_2O_2 (c) AlCrFeCoNi and H_2O_2 and (d) photodegradation efficiency of RhB in various pH reaction.

[3] Carmen, Z., Daniel, S. (2012). Textile Organic Dyes – Characteristics, Polluting Effects and Separation/Elimination Procedures from Industrial Effluents – A Critical Overview. In: Tomasz, P., Mostrag-Szlichtyng, A. (eds.). *Organic Pollutants Ten Years After the Stockholm Convention - Environmental and Analytical Update*. InTech. DOI: 10.5772/32373.

[4] Benkhaya, S., M'rabet, S., El Harfi, A. (2020). Classifications, properties, recent synthesis and applications of azo dyes. *Heliyon*, 6, e03271. DOI: 10.1016/j.heliyon.2020.e03271.

[5] Akpan, U.G., Hameed, B.H. (2009). Parameters affecting the photocatalytic degradation of dyes using TiO_2-based photocatalysts: A review. *Journal of Hazardous Materials*, 170(2–3), 520–529. DOI: 10.1016/j.jhazmat.2009.05.039.

[6] Balanosky, E. (2000). Oxidative degradation of textile waste water. Modeling reactor performance. *Water Research*, 34(2), 582–596. DOI: 10.1016/S0043-1354(99)00150-5.

[7] Schrank, S.G., Dos, Santos, J.N.R., Souza, D.S., Souza, E.E.S. (2007). Decolourisation effects of Vat Green 01 textile dye and textile wastewater using H_2O_2/UV process. *Journal of Photochemistry and Photobiology A: Chemistry*, 186, 125–129. DOI: 10.1016/j.jphotochem.2006.08.001.

[8] Saeed, M., Adeel, S., Shahzad, M.A., Muneer, M., Younas, M. (2014). Pt/Al_2O_3 Catalyzed Decolorization of Rhodamine B Dye in Aqueous Medium. *Chiang Mai Journal of Science*, 42(3), 730–744.

[9] Wang, X., Pan, Y., Zhu, Z., Wu, J. Efficient degradation of rhodamine B using Fe-based metallic glass catalyst by Fenton-like process. *Chemosphere*, 117, 638–643. DOI: 10.1016/j.chemosphere.2014.09.055.

[10] Wang, X., Zhang, Q., Liang, S.-X., Jia, Z., Zhang, W., Wang, W., Zhang, L.-C. (2020). Fe-Based Metallic Glasses and Dyes in Fenton-Like Processes: Understanding Their Intrinsic Correlation. *Catalysts*, 10, 48. DOI: 10.3390/catal10010048.

[11] Cantor, B., Chang, I.T.H., Knight, P., Vincent, A.J.B. (2004). Microstructural development in equiatomic multicomponent alloys. *Materials Science and Engineering A*, 375–377, 213–218. DOI: 10.1016/j.msea.2003.10.257.

[12] Kumar, A., Singh, A., Suhane, A. (2022). Synthesis and characterization of a novel CoCrFeMnNi high-entropy alloy-reinforced AA6082 composite. *Journal of Materials Research*, 37, 2961–2978. DOI: 10.1557/s43578-022-00701-3

[13] Gorsse, S., Couzinié, J.-P., Miracle, D.B. From high-entropy alloys to complex concentrated alloys. *Comptes Rendus Physique*, 19, 721–736. DOI: 10.1016/j.crhy.2018.09.004.

[14] Simić, L., Stopic, S., Friedrich, B., Zadravec, M., Jelen, Ž., Bobovnik, R., Anžel, I., Rudolf, R. (2022). Synthesis of Complex Concentrated Nanoparticles by Ultrasonic Spray Pyrolysis and Lyophilisation. *Metals*, 12, 1802. DOI: 10.3390/met12111802.

[15] Zhang, X., Liang, J., Sun, Y., Zhang, F., Li, C., Hu, C., Lyu, L. Mesoporous reduction state cobalt species-doped silica nanospheres: An efficient Fenton-like catalyst for dual-pathway degradation of organic pollutants. *Journal of Colloid and Interface Science*, 576, 59–67. DOI: 10.1016/j.jcis.2020.05.007.

[16] Wang, N. (2022). FeCoNiMnCuTi high entropy amorphous alloys and M50Ti50 (M = Fe, Cu, FeCoNiMnCu) amorphous alloys: Novel and efficient catalysts for heterogeneous photo-Fenton decomposition of Rhodamine B. *Surfaces and Interfaces*, 33, 102265. DOI: 10.1016/j.surfin.2022.102265.

[17] Koundinya, N.T.B.N., Babu, C.S., Sivaprasad, K., Susila, P., Babu, N.K., Baburao, J. (2013). Phase Evolution and Thermal Analysis of Nanocrystalline AlCrCuFeNiZn High Entropy Alloy Produced by Mechanical Alloying. *Journal of Materials Engineering and Performance*, 22, 3077–3084. DOI: 10.1007/s11665-013-0580-5.

[18] Zhao, Y., Cao, S., Zeng, L., Xia, M., Jakse, N., Li, J. (2023). Intermetallics in Ni–Al Binary Alloys: Liquid Structural Origin. *Metallurgical and Materials Transactions A*, 54, 646–657. DOI: 10.1007/s11661-022-06910-z.